Supplemental Material can be found at:
http://www.jlr.org/content/suppl/2005/12/01/M400462-JLR200.DC2.html
http://www.jlr.org/content/suppl/2005/05/18/M400462-JLR200.DC1.html

# Changes in gene expression associated with loss of function of the NSDHL sterol dehydrogenase in mouse embryonic fibroblasts[S]

**David Cunningham,* Daniel Swartzlander,* Sandya Liyanarachchi,† Ramana V. Davuluri,† and Gail E. Herman[1,*,§]**

Center for Molecular and Human Genetics, Columbus Children's Research Institute,* Division of Human Cancer Genetics, Comprehensive Cancer Center,† and Department of Pediatrics,§ Ohio State University, Columbus, OH

**Abstract Seven human disorders of postsqualene cholesterol biosynthesis have been described. One of these, congenital hemidysplasia with ichthyosiform nevus and limb defects (CHILD) syndrome, results from mutations in the X-linked gene NADH sterol dehydrogenase-like (*NSDHL*) encoding a sterol dehydrogenase. A series of mutant alleles of the murine *Nsdhl* gene are carried by bare patches (*Bpa*) mice, with $Bpa^{1H}$ representing a null allele. Heterozygous $Bpa^{1H}$ females display skin and skeletal abnormalities in a distribution reflecting random X inactivation, whereas hemizygous male embryos die before embryonic day 10.5. To investigate the molecular basis of defects associated with perturbations in cholesterol biosynthesis, microarray analysis was performed comparing gene expression in embryonic fibroblasts expressing the $Bpa^{1H}$ allele versus wild-type (*wt*) cells. Labeled cDNAs from cells grown in normal serum or lipid-depleted serum (LDS) were hybridized to microarrays containing 22,000 mouse genes. Among 44 genes that showed higher expression in the $Bpa^{1H}$ versus *wt* cells grown in LDS, 11 function in cholesterol biosynthesis, 7 are involved in fatty acid synthesis, 3 (*Srebp2*, *Insig1*, and *Orf11*) encode sterol-regulatory proteins, and 2 (*Ldlr* and *StarD4*) are lipid transporters. Of the 21 remaining genes, 16 are known genes, some of which have been implicated previously in cholesterol homeostasis or lipid-mediated signaling, and 5 are uncharacterized cDNA clones.**—Cunningham, D., D. Swartzlander, S. Liyanarachchi, R. V. Davuluri, and G. E. Herman. **Changes in gene expression associated with loss of function of the NSDHL sterol dehydrogenase in mouse embryonic fibroblasts. *J. Lipid Res.* 2005.** 46: **1150–1162.**

**Supplementary key words** cholesterol biosynthesis • congenital hemidysplasia with ichthyosiform nevus and limb defects syndrome • microarray • bare patches • sterol • development

Cholesterol homeostasis in mammalian cells is achieved, in part, through coordinated regulation of the ~30 enzymatic reactions that constitute the cholesterol biosynthetic pathway. Primary regulation of the pathway occurs by sterol-mediated feedback of transcription of the genes encoding cholesterogenic enzymes (reviewed in 1). Post-transcriptional mechanisms have also been described, including the regulated degradation in the endoplasmic reticulum (ER) of HMG-CoA reductase (HMGR), which catalyzes the rate-limiting step in the pathway (2). Further control involves regulation of the cellular uptake, efflux, and sites of storage of cholesterol within the cell (3).

The precision with which cholesterol homeostasis is achieved and maintained may be attributable to its potentially deleterious effects on the organism when levels are increased and the tremendous energy expenditure involved in its de novo production. Most important, however, cholesterol is an essential constituent of cell membranes. Localized regions of increased cholesterol in the plasma membrane help define lipid rafts and caveolae that function in intercellular signaling and endocytosis, respectively (4). Covalent modification of active hedgehog proteins by cholesterol to provide membrane anchoring is required for their proper signaling functions during embryonic development (5). Furthermore, cholesterol is the precursor for the synthesis of steroid hormones and bile acids.

Abbreviations: *Bpa*, bare patches; CHILD, congenital hemidysplasia with ichthyosiform nevus and limb defects; 7DHC, 7-dehydrocholesterol; E13.5, embryonic day 13.5; ER, endoplasmic reticulum; FACS, fluorescence-activated cell sorting; GFP, green fluorescent protein; HMGR, 3-hydroxy-3-methylglutaryl-CoA reductase; LDS, lipid-depleted serum; MEF, mouse embryonic fibroblast; NSDHL, NADH sterol dehydrogenase-like; SCAP, sterol-regulatory element binding protein cleavage-activating protein; SREBP, sterol-regulatory element binding protein; *wt*, wild type.

[1] To whom correspondence should be addressed.
e-mail: hermang@pediatrics.ohio-state.edu

[S] The online version of this article (available at http://www.jlr.org) contains an additional three tables.

*Manuscript received 17 November 2004 and in revised form 1 February 2005 and in re-revised form 17 March 2005.*

*Published, JLR Papers in Press, April 1, 2005.*
*DOI 10.1194/jlr.M400462-JLR200*

Copyright © 2005 by the American Society for Biochemistry and Molecular Biology, Inc.



**This article is available online at http://www.jlr.org**

Downloaded from www.jlr.org by guest, on June 14, 2012

Supplemental Material can be found at:
http://www.jlr.org/content/suppl/2005/12/01/M400462-JLR200.DC2.html
http://www.jlr.org/content/suppl/2005/05/18/M400462-JLR200.DC1.html

During the past decade, seven human developmental malformation syndromes have been identified that arise from mutations in genes encoding enzymes that function in the postsqualene steps of cholesterol biosynthesis (6, 7). These disorders are marked by several common features, including growth and mental retardation, major developmental malformations, and skeletal defects. However, they are distinguished by their incidence and severity, following a general trend of decreasing incidence and increasing severity, including prenatal lethality, for genes that function in earlier steps of the pathway. It has been suggested that deficiency of cholesterol or total sterols, toxicity from the excessive accumulation of specific sterol intermediates, distinct effects on hedgehog protein modification and signaling, and abnormal feedback regulation of early steps in the pathway, with concomitant effects on isoprenoids that are generated as side products, all may contribute to the observed phenotypes and disease pathogenesis.

Spontaneous mouse mutants or animals generated by targeted gene disruption exist for six of the seven human disorders, providing potential models to examine disease pathogenesis (7, 8). One of these mouse models is the X-linked, male-lethal bare patches (*Bpa*) mouse resulting from mutations in the NADPH steroid dehydrogenase-like (*Nsdhl*) gene (9). *Nsdhl* encodes a ubiquitously expressed 362 amino acid protein that functions as a 3β-hydroxysterol dehydrogenase and is involved in the removal of C-4 methyl groups at an intermediate step in the conversion of lanosterol to cholesterol. The gene was first identified by positional cloning in the mouse. Subsequently, mutations in human *NSDHL* were discovered in patients with congenital hemidysplasia with ichthyosiform nevus and limb defects (CHILD) syndrome, an extremely rare X-linked, male-lethal malformation syndrome associated with unilateral ichthyosiform skin lesions and limb reduction defects (10, 11).

All of the seven known mutant murine *Nsdhl* alleles produce a characteristic striping of the coat in heterozygous females that follows the lines of X inactivation, and all of the mutations are lethal by embryonic day 13.5 (E13.5) in hemizygous males (9, 12, 13). The $Bpa^{1H}$ allele, resulting from the nonsense mutation K103X, produces the most severe phenotype in surviving females, with asymmetric dwarfing and skeletal dysplasia, early postnatal patchy hyperkeratotic skin eruptions, and occasional microphthalmia and/or cataracts. The majority of hemizygous $Bpa^{1H}$ males die by E9.5. Evidence from sterol analyses of affected male embryos for two less severe *Nsdhl* alleles suggests that the male lethality is not attributable to simple cholesterol deficiency, because cholesterol and total sterol levels in affected male embryos are comparable to those of wild-type (*wt*) littermates, probably as a result of maternal transfer across the placenta (13).

To begin to examine the cellular consequences of an enzymatic block in cholesterol synthesis at the level of the sterol C-4 demethylase complex, we have isolated mouse embryonic fibroblasts (MEFs) from $Bpa^{1H}$ embryos. We describe here comparisons of gene expression profiles from mutant and normal MEFs using microarray and real-time PCR analyses.

## MATERIALS AND METHODS

### Mice

A breeding stock of $Bpa^{1H}$ mice (9) was maintained by mating heterozygous $Bpa^{1H}$ females to F1 hybrid C57BL/6J$A^{w\text{-}J}$×CBA/CaGnLe males (Jackson Laboratory, Bar Harbor, ME). The green fluorescent protein (GFP) transgenic line TgN(GFPX)4Nagy (strain D4/XEGFP) on a 129/Sv background (14, 15) was obtained from Dr. David Burke (University of Michigan). To minimize skewing of X inactivation in heterozygous females, the GFP transgene was recombined onto a C57BL/6 X chromosome carrying an $Xce^b$ allele (16, 17) by backcrossing an F1 hybrid TgN(GFPX)4Nagy×C57BL/6 female to a C57BL/6 male. Female N2 offspring were genotyped for *Xce* by PCR using the linked microsatellite markers *DXPas28* and *DXPas29* that distinguish the C57BL/6 $Xce^b$ allele from the 129 $Xce^a$ allele (16). Backcrossing of GFP-positive females that were homozygous for $Xce^b$ to C57BL/6J males was continued to N5.

### Generation and culture of primary murine embryonic fibroblasts

To generate primary cultures of embryonic fibroblasts, $Bpa^{1H}$ females were mated to a backcross N5 GFP transgenic male. Pregnant females were sacrificed at E15.5, and yolk sac DNA was purified for PCR genotyping of the embryos. The sex of the embryos was determined using primers for *Smcx* as described previously (18), and *Nsdhl* genotype was inferred using the closely linked microsatellite *DXMit1* (19).

All tissue culture reagents were purchased from Invitrogen Life Technologies (Carlsbad, CA) unless stated otherwise. After removing the head and internal organs, the embryos were minced and incubated for 30 min at 37°C in 1 mg/ml collagenase A (Roche Applied Science, Indianapolis, IN) dissolved in MEMα medium. The disaggregated cells were pelleted by centrifugation and plated at $5 \times 10^5$ cells/75 cm flask in MEMα supplemented with 10% FBS (Hy-Clone, Logan, UT), penicillin, streptomycin, and 2 mM L-glutamine. Cells were grown at 37°C in a 5% $CO_2$ atmosphere and replated at $5 \times 10^5$ cells/flask every 3 days.

Lipid-depleted serum (LDS) was prepared by adding 2 mg of silicon dioxide (Cab-O-Sil™ M-5; Acros, Morris Plains, NJ) to 100 ml of FBS and stirring overnight at 4°C (20). The serum was passed through a 0.2 μM sterile filter, and 15 mg of insulin-transferrin-sodium selenite media supplement (catalog number I 1884; Sigma, St. Louis, MO) was added per 100 ml of serum. The treated serum was 97% cholesterol-depleted as determined using the Infinity™ cholesterol assay (Thermo Electron Corp., Waltham, MA).

MEFs that expressed GFP were counted using a Coulter EpicsXL flow cytometer equipped with EXPO32 acquisition and analysis software (Beckman Coulter, Fullerton, CA). GFP-negative (GFP−) cells were sorted from mixed populations of heterozygous female MEFs at passage 3 using a FACSVantage DiVa instrument (BD Biosciences, San Jose, CA). Sorted cells were plated at $5 \times 10^5$/75 cm flask and replated when they reached confluence after 4 days. Subconfluent cultures of MEFs at passage 5 were used for microarray analysis. For growth in LDS, cells were first grown in normal medium for 24 h after replating, then rinsed twice with PBS, and LDS medium was added. Incubation in LDS medium was continued at 37°C for 24, 36, or 48 h, at which time the cells were harvested for RNA isolation.

Downloaded from www.jlr.org by guest, on June 14, 2012

Supplemental Material can be found at:
http://www.jlr.org/content/suppl/2005/12/01/M400462-JLR200.DC2.html
http://www.jlr.org/content/suppl/2005/05/18/M400462-JLR200.DC1.html

### RT-PCR, sequencing, and microarrays

Total RNA was isolated from MEFs at passage 5 using TRIzol Reagent (Invitrogen, Carlsbad, C) according to the manufacturer's protocol. RNA was further purified using an RNeasy Mini Kit (Qiagen, Valencia, CA). The quality and concentration of RNA samples were assayed using an Agilent 2100 Bioanalyzer (Agilent Technologies, Palo Alto, CA). RT-PCR and DNA sequencing of cDNA to test for the monoallelic expression of *Nsdhl* in sorted cell populations were performed as described (21) using a forward primer from exon 2 (NsdhlE2F, 5′-CCAGCTGATCATGGTGAATC-3′) and a reverse primer from exon 5 (NsdhlE5R, 5′-TGGCACTGCTGGTTAAAATGAGTTT-3′), generating a 400 bp PCR product that spans the site of the *Bpa*$^{1H}$ mutation in exon 4.

For microarray analysis, cDNA was synthesized from 40 μg of total RNA using amino-allyl dUTP (Sigma), and either Cy3 or Cy5 dye (Amersham Biosciences, Piscataway, NJ) was then conjugated to the cDNA samples (22). Approximately 0.5 μg of purified target cDNAs from mutant and *wt* cells was combined with control target cDNAs in 500 μl of hybridization buffer (In Situ Hybridization Kit Plus; Agilent Technologies) and hybridized to glass slide microarrays containing 60-mer oligonucleotides representing ~22,000 mouse gene sequences (Mouse Development Oligo Microarray; Agilent Technologies). Hybridizations were performed with constant rotation in Agilent hybridization chambers for 16 h at 60°C. Slides were washed in 6× SSC (1× SSC is 150 mM sodium chloride, 15 mM sodium citrate) with 0.005% Triton X-102 for 10 min at room temperature and in ice-cold 0.1× SSC, 0.0005% Triton X-102 for 5 min. Fluorescence signal was quantified using an Affymetrix 428 Array Scanner (Affymetrix, Santa Clara, CA) and GenePix 4.0 software (Axon Instruments, Union City, CA).

A total of 15 microarray experiments were performed, each involving cohybridization of *wt* and *Bpa*$^{1H}$ cDNA samples from littermates. Six primary cultures of sorted GFP− MEFs from three different litters were used and designated 1W, 1B, 2W, 2B, 3W, and 3B, where the number specifies the litter and W or B signifies MEFs expressing the *wt* or *Bpa*$^{1H}$ *Nsdhl* allele, respectively. Five experiments (four with 1W vs. 1B and one with 3W vs. 3B) were performed with RNA from cells grown in normal medium; four experiments (two using 1W vs. 1B, one using 2W vs. 2B, and one using 3W vs. 3B) included RNA from cells grown in LDS for 24 h; two experiments (one using 1W vs. 1B and one using 3W vs. 3B) included samples from cells grown in LDS for 36 h; and four experiments (three using 1W vs. 1B and one using 3W vs. 3B) contained RNA from cells grown in LDS for 48 h. Independently isolated RNA samples were used in all of the experiments except two, one in normal medium and one after 48 h in LDS, in which the same RNA sample pairs, 1W and 1B with reversed Cy3 and Cy5 labeling, were hybridized to different microarrays.

Statistical analysis of microarray data was performed using the software package S-Plus version 6.2.1 (Insightful Corp., Seattle, WA). Before statistical analysis, the median of the background corrected fluorescence intensities of the two dyes (Cy3 and Cy5), as well as the ratios of the median intensities of the two dyes, were calculated for each spot on the array. Array spots were screened for poor quality or low signal intensity compared with the local background (% > B635 + 2SD < 25 for the Cy5 channel and % > B532 + 2SD < 25 for the Cy3 channel), and those identified were excluded from the analysis and treated as missing values (denoted NA in supplementary Tables I and II). Array data sets were then normalized using an intensity-dependent normalization method by fitting a locally weighted least-square fit (LOWESS) to the M versus A plot, where M = log intensity ratio $\log_2$ (Cy3/Cy5) and A = mean log intensity $\log_2$ (Cy3 × Cy5)$^{1/2}$ (23). Data for color inversion experiments were combined and averaged as a single experiment. A one-sample *t*-test was performed to identify upregulated or downregulated genes in the *Bpa*$^{1H}$ cells compared with the *wt* cells for replicate experiments from each growth condition time point separately, as well as for the three LDS time points combined, under the null hypothesis that the mean log ratio of test over reference is zero. Cluster analysis was performed using GeneCluster software, and the results were displayed graphically using TREEVIEW version 1.60 software (24). Microarray probes that met the following criteria were included in the cluster analysis: they showed a mean fold difference between the *Bpa*$^{1H}$ and *wt* signal greater than 1.5 for at least one of the experimental time points with a *P* value of less than 0.1, and there were less than 80% missing values in the 13 experiments.

To identify the most consistent and statistically significant differences in gene expression between *Bpa*$^{1H}$ and *wt* cells associated with lipid depletion, data from the three LDS time point experiments (24, 36, and 48 h) were combined. Although the yield of RNA from samples from the 48 h time point was lower than from the other time points, there was no difference in the quality of the 48 h RNA samples, as determined by analysis on the Bioanalyzer. *P* values were assigned to genes that displayed a mean fold difference of greater than 1.5 and had less than 50% missing values for the nine LDS experiments. Lists of all of the upregulated and downregulated microarray probes, ranked by *P* value, with the calculated fold difference in individual experiments expressed as a $\log_2$ value, as well as the mean fold difference and *P* values calculated for the combined LDS experiments, are provided in supplementary Tables I and II.

### Real-time PCR

cDNA was synthesized from 20 μg of total RNA from MEFs using SuperScript II reverse transcriptase with oligo-dT and random hexamer primers (Invitrogen) using standard protocols. After cDNA samples were brought to a final volume of 200 μl in water, a dilution series of 1:2, 1:4, and 1:8 was made for each sample, and aliquots were stored at −20°C. Amplification reactions included 2 μl of cDNA with 0.5 μM forward and reverse primers in SYBR Green PCR Master Mix (Applied Biosystems, Foster City, CA) in a total volume of 25 μl. Primers were designed to span introns if possible and to generate PCR products between 80 and 120 bp. Primer sequences are provided in supplementary Table III. Real-time PCR amplification was performed using an ABI Prism 7700 Sequence Detector equipped with Sequence Detector version 1.6.3 software (Perkin Elmer, Wellesley, MA) for data acquisition and analysis. Amplification reactions of the three cDNA dilutions (1:2, 1:4, and 1:8) were performed in parallel, and the results using the cDNA from *wt* MEFs grown in normal medium were used to generate a standard curve for each primer pair. The relative signal quantity for the remaining samples was calculated using this standard curve. RNA samples were analyzed from two *Bpa*$^{1H}$ (1B and 3B) and two *wt* (1W and 3W) cultures of sorted MEFs, each of which had been grown in either normal medium or LDS medium for 24 h. RNA aliquots from MEF cultures 3B and 3W were from the same samples used for microarray analysis, whereas RNAs from 1B and 1W were isolated from independent cultures of these cells.

## RESULTS

### Generation of *Bpa*$^{1H}$ mutant fibroblasts

The *Bpa*$^{1H}$ allele of *Nsdhl* was chosen for microarray analysis because it is predicted to be null and has the most severe phenotype among the known murine mutations (12).



Downloaded from www.jlr.org by guest, on June 14, 2012

Supplemental Material can be found at:
http://www.jlr.org/content/suppl/2005/12/01/M400462-JLR200.DC2.html
http://www.jlr.org/content/suppl/2005/05/18/M400462-JLR200.DC1.html

We chose to compare gene expression profiles from primary cultured embryonic fibroblasts rather than embryonic tissue(s) for several reasons. As with many lethal mutants, *Bpa*$^{1H}$ male embryos exhibit a range of early postimplantation defects, likely rendering the effects of the mutation difficult to resolve from the biological "noise" caused by the rapidly changing normal developmental patterns of gene expression at this stage. Second, cultured cells provide a relatively simple system that is amenable to manipulations, such as growth in LDS. Finally, because the skin of heterozygous females is one of the tissues affected by all of the known mutant *Nsdhl* alleles, fibroblasts, the major cell type populating the dermis of the skin, represent an "affected" cell type for investigating the defects seen in *Bpa* mice.

The early lethality of affected *Bpa*$^{1H}$ male embryos, however, prohibited the expansion of sufficient viable MEFs for our experiments. We circumvented this problem by taking advantage of the phenomenon of random and stable X inactivation in mammalian females as follows: *Bpa*$^{1H}$ females were mated to males carrying a ubiquitously expressed X-linked GFP transgene [TgN(GFPX)4Nagy] that undergoes normal, random inactivation in the early postimplantation female embryo (14). Resulting female embryos all carried a paternally inherited X chromosome with a GFP transgene and *wt Nsdhl* allele, but they expressed both in approximately half of their cells as a result of random X inactivation. The remaining cells expressed a maternal *Bpa*$^{1H}$ or *wt Nsdhl* allele, depending on which X chromosome was inherited from the *Bpa*$^{1H}$ dam (**Fig. 1**).

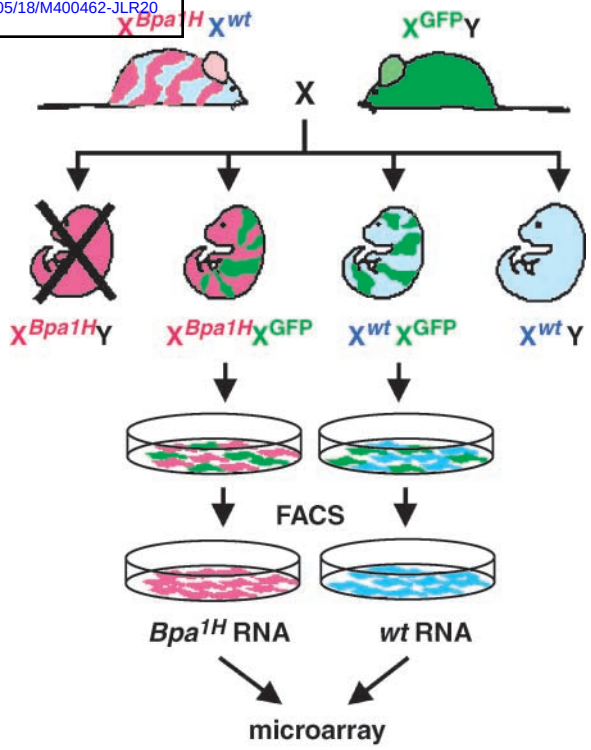


**Fig. 1.** Experimental strategy for microarray analysis of bare patches (*Bpa*$^{1H}$) mouse embryonic fibroblasts (MEFs). Females heterozygous for the *Bpa*$^{1H}$ mutant allele of the X-linked NADPH steroid dehydrogenase-like (*Nsdhl*) gene were crossed with TgN(GFPX)4Nagy males that carry a ubiquitously expressed, X-linked green fluorescent protein (GFP) transgene. Hemizygous *Bpa*$^{1H}$ male embryos die by embryonic day 10.5 (E10.5). MEFs were cultured from female embryos sacrificed at E15.5. The sex and *Nsdhl* genotypes of the embryos were determined by PCR assays of yolk sac DNA (see Materials and Methods). Because of normal X inactivation, each culture was a mixed population of GFP-positive (GFP+) cells and GFP-negative (GFP−) cells that expressed either the *Bpa*$^{1H}$ allele or the wild-type (*wt*) allele of *Nsdhl*. GFP− cells were isolated by fluorescence-activated cell sorting (FACS) at passage 3, generating >99% pure populations of *Bpa*$^{1H}$ or *wt* MEFs. Total RNA from these cultures was isolated at passage 5 after defined periods of growth in either normal or lipid-depleted serum (LDS) medium and used to synthesize fluorescently labeled cDNAs that were cohybridized to mouse oligonucleotide microarrays.

After primary cultures of female MEFs were established from genotyped E15.5 embryos, the relative abundance of cells expressing GFP (GFP+) and not expressing GFP (GFP−) was measured by flow cytometry (**Fig. 2A**). The GFP+ and GFP− cells were detected as two well-defined peaks, with few cells showing an intermediate level of fluorescence. The ratio of GFP+ to GFP− cells, when measured after initial expansion at passage 1, varied among the different cultures but did not correlate with the *Nsdhl* allele, mutant or *wt*, present on the GFP− X chromosome. The proportion of GFP+ cells in cultures from eight heterozygous *Bpa*$^{1H}$ female embryos from four litters ranged from 24% to 82% (mean = 47 ± 21%), whereas GFP+ cells in cultures from six embryos homozygous for *wt Nsdhl* ranged from 27% to 54% (mean = 41 ± 10%). The ratios seen in early-passage MEFs did not change significantly after nine passages in culture (data not shown), further suggesting that the mutant cells grow as well as *wt* cells in a mixed population under standard culture conditions.

Only GFP− cells were used in our analyses, to exclude any effects that might be produced by long-term GFP expression. The GFP− cells were sorted by fluorescence-activated cell sorting (FACS) to a purity of >99% from both mutant and *wt* passage 3 MEFs. Sorted cells retained this level of purity through at least passage 9 (Fig. 2B). Purity was also assessed by sequencing *Nsdhl* exon 4, which includes the *Bpa*$^{1H}$ mutation, in PCR-amplified cDNA synthesized from sorted mutant GFP− cells. As shown in Fig. 2C, these cells expressed only the mutant allele, as demonstrated by the presence of the thymidine peak at nucleotide 522. Control GFP− cells from *wt* embryos showed the expected adenosine peak (Fig. 2D). Control experiments in which known amounts of mutant and *wt Nsdhl* PCR products were mixed and sequenced indicated that as little as 5% of a variant sequence is detectable as a superimposed peak at nucleotide 522 on the sequence trace data (data not shown). To verify that the *wt Nsdhl* allele on the GFP X chromosome had been stably silenced in cells, after eight passages in culture, sorted GFP− MEFs were retested by flow cytometry and RT-PCR. Less than 1% of the cells were GFP+, and *wt Nsdhl* mRNA could not be detected by sequencing the *Nsdhl* RT-PCR product from the *Bpa*$^{1H}$ cells (data not shown), consistent with the expected



Downloaded from www.jlr.org by guest, on June 14, 2012

Supplemental Material can be found at:
http://www.jlr.org/content/suppl/2005/12/01/M400462-JLR200.DC2.html
http://www.jlr.org/content/suppl/2005/05/18/M400462-JLR200.DC1.html

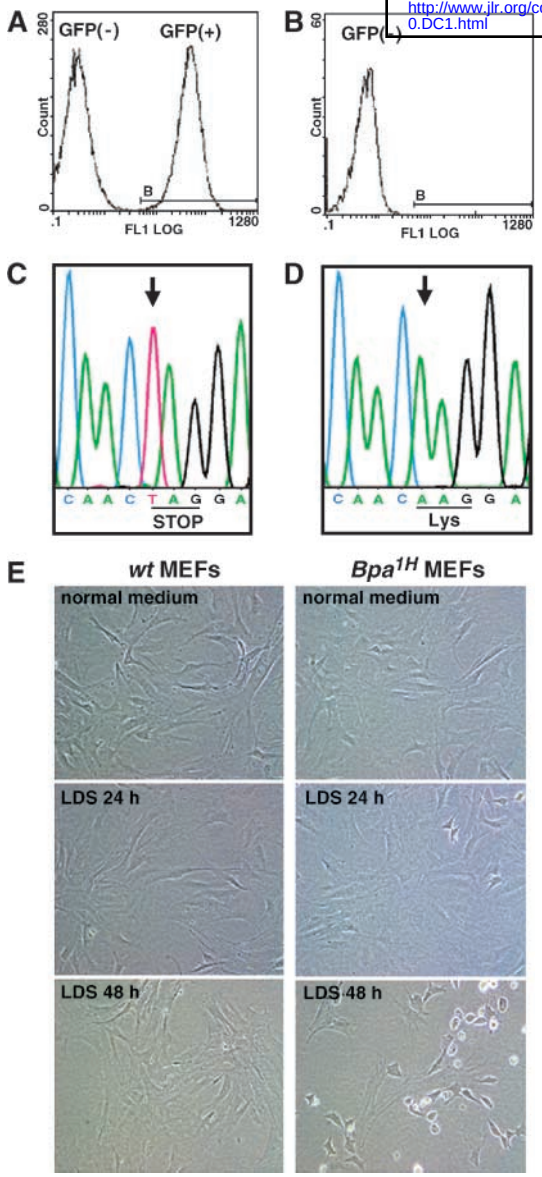


**Fig. 2.** Characteristics of *Bpa*$^{1H}$ and *wt* MEFs. A: Quantitation of GFP+ and GFP− cells by flow cytometry in a typical population of unsorted female MEFs at passage 1. GFP signal is shown on the *x* axis, with cell number indicated on the *y* axis. Note the two well-defined peaks of signal that enabled cell sorting of GFP− cells to a high degree of purity. B: Detection of GFP+ and GFP− cells by flow cytometry in a population of female MEFs at passage 9 that had been sorted as GFP− at passage 3. Less than 1% of the cells were GFP+, indicating that sorting was efficient and that the GFP transgene was stably silenced by X inactivation. C: Partial sequence of *Nsdhl* exon 4 near nucleotide 522 (arrow) in cDNA synthesized from total RNA isolated from sorted *Bpa*$^{1H}$ MEFs, showing the thymidine residue that results in the nonsense mutation. No evidence of an overlapping adenosine peak, indicative of *wt Nsdhl* expression, was detected. D: Sequence of the same region of *Nsdhl* shown in C in cDNA derived from sorted *wt* MEFs showing the expected lysine-103 codon. E: Phase-contrast microscopy images of sorted *wt* and *Bpa*$^{1H}$ MEFs at passage 5 grown in normal medium or LDS medium for 24 and 48 h. Both cultures grew at similar rates in normal medium and appeared morphologically similar after 24 h in LDS medium. However, after 48 h in LDS medium, many of the *Bpa*$^{1H}$ MEFs had rounded up and detached from the substrate, whereas the *wt* cells continued to grow normally. Cells are shown at 200× magnification.

stable and complete silencing of both GFP and the *wt Nsdhl* allele on the inactive X chromosome.

Under standard culture conditions, the *Bpa*$^{1H}$ and *wt* cells were essentially indistinguishable in terms of morphology and growth rate. Because the *Bpa*$^{1H}$ cells would be expected to be fully dependent on the uptake of exogenous cholesterol from the culture medium, we compared the growth of parallel cultures of *wt* and *Bpa*$^{1H}$ cells in medium supplemented with LDS (Fig. 2E). After 24 h in LDS medium, the appearance of the two cultures was roughly equivalent. However, at 36 h, some of the mutant cells had rounded up and detached from the surface, and by 48 h in LDS medium, approximately half as many *Bpa*$^{1H}$ cells as *wt* cells could be seen attached to the surface, presumably as a result of cell death caused by cholesterol deficiency. The *wt* cells showed little to no cell death in LDS medium and subsequently grew to confluence at a normal rate.

### Microarray analysis

RNA samples were isolated from three independent pairs of early-passage, sorted, primary cell cultures of *Bpa*$^{1H}$ and *wt* MEFs grown in both normal medium and LDS medium (see Materials and Methods). Because the *Bpa*$^{1H}$ MEFs appeared to grow normally in standard medium, we reasoned that the effects of the mutation on global gene expression might be more readily detectable under conditions of cholesterol deprivation. We chose three time points of growth in LDS medium (24, 36, and 48 h), because the observed cell death of the mutant MEFs over time would be expected to result in increasing secondary effects on gene expression associated with apoptosis or altered cell cycle regulation. In contrast, altered expression patterns in early time points or in all of the time points might reflect effects that were more directly related to *Nsdhl* loss of function.

Fluorescently labeled cDNA samples derived from mutant and *wt* RNA were cohybridized to oligonucleotide arrays (Agilent Mouse Development) representing ~22,000 mouse genes from the NIA 15k and 7.4k cDNA clone sets (25). A total of 15 hybridizations representing 13 independent experiments and data sets comparing *Bpa*$^{1H}$ versus *wt* RNA were performed: five with cells grown in normal medium, four with cells in LDS medium for 24 h, two with cells in LDS medium for 36 h, and four with cells grown in LDS medium for 48 h (see Materials and Methods). To gain an overview of the microarray results, cluster analysis was performed on ~1,525 genes that showed at least 1.5-fold higher or lower expression with $P < 0.1$ in the *Bpa*$^{1H}$ MEFs relative to *wt* cells in at least one of the time points (data not shown). One cluster, which included 25 genes, was characterized by upregulation of expression in the mutant cells in all three LDS time points relative to samples grown in normal medium (**Fig. 3A**). Not surprisingly, most of the genes in this cluster are known to be directly involved in cholesterol synthesis or in its regulation. In contrast, another cluster was characterized by genes that showed the greatest change in expression only in the samples from 48 h in LDS medium. It

Downloaded from www.jlr.org by guest, on June 14, 2012

Supplemental Material can be found at:
http://www.jlr.org/content/suppl/2005/12/01/M400462-JLR200.DC2.html
http://www.jlr.org/content/suppl/2005/05/18/M400462-JLR200.DC1.html

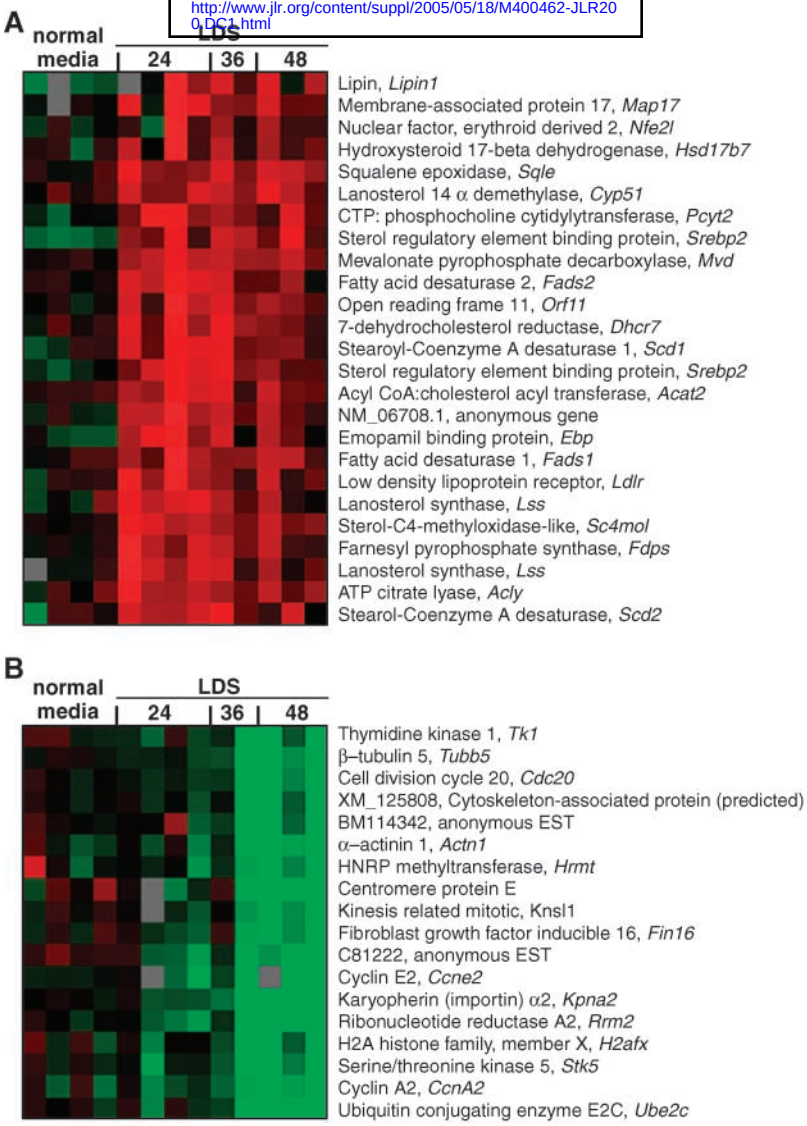


**Fig. 3.** Selected clusters of genes demonstrating similar patterns of differential expression between *Bpa*$^{1H}$ and *wt* MEFs. Each column represents a different experiment in which cells were cultured in either normal medium or LDS medium for 24, 36, or 48 h. Cluster analysis was performed using GeneCluster and TREEVIEW software (24) on 1,525 genes that showed a mean fold difference of at least 1.5 between mutant and *wt* cells in at least one experimental time point (see Materials and Methods). Red indicates higher expression in the *Bpa*$^{1H}$ cells; green represents lower expression in the *Bpa*$^{1H}$ cells; black indicates no difference between the *Bpa*$^{1H}$ and *wt* cells; and gray indicates no data available because of low signal or poor spot quality. A: A cluster of 25 genes that was characterized by higher expression in *Bpa*$^{1H}$ versus *wt* MEFs at all three time points of growth in LDS. B: A cluster of 18 genes that showed a profile of lower expression in the *Bpa*$^{1H}$ compared with *wt* cells with longer culture times in LDS medium.

included several genes that are involved in cell cycle control, such as *Cdc20*, *Ccne2*, and *CcnA2*, probably reflecting deleterious secondary effects of cholesterol deficiency that accumulate over time (Fig. 3B).

Genes that showed differential expression of at least 1.5-fold between *Bpa*$^{1H}$ and *wt* cells were then ranked using a more stringent *P* value of $<0.001$ for each experimental time point to assess the most significant patterns. By this criterion, for cells grown in normal medium, only one gene was identified as upregulated in the mutant versus *wt* cells and two were downregulated. The upregulated gene was an anonymous cDNA of unknown function (GenBank accession number BM118718). The downregulated genes were *Nsdhl* itself and *Ywhaz*, encoding 14-3-3ζ, a multifunctional regulator of phosphoproteins (26, 27). The lower level of *Nsdhl* transcript in the *Bpa*$^{1H}$-expressing cells may be a result of accelerated decay of the message attributable to premature termination of translation caused by the nonsense mutation (28). Based on searches of mouse expressed sequence tag databases (University of California Santa Cruz Genome Browser, http://genome.ucsc.edu/, mouse genome May 4, 2004 assembly), the oligo probe for *Ywhaz* (Agilent feature A_65_P09812) apparently represents sequence from the 3′ untranslated region of a rare



Downloaded from www.jlr.org by guest, on June 14, 2012

Supplemental Material can be found at:
http://www.jlr.org/content/suppl/2005/12/01/M400462-JLR200.DC2.html
http://www.jlr.org/content/suppl/2005/05/18/M400462-JLR200.DC1.html

alternative transcript that extends the message ~500 bp and uses a downstream polyadenylation signal. The functional significance of this, or several other variant *Ywhaz* transcripts with alternative 5′ and 3′ untranslated regions, is not known. A separate oligo probe from the coding region of *Ywhaz* (Agilent feature A_65_P13182) showed no significant differences between *Bpa*$^{1H}$ and *wt* samples, suggesting that the majority of *Ywhaz* message was unaffected in the mutant cells.

Of those genes identified as upregulated in *Bpa*$^{1H}$ versus *wt* samples from the three time points of growth in LDS medium, a majority were involved in lipid metabolism. When the data for all three time points in LDS were combined and analyzed together, 44 genes had *P* values of $<0.001$ (**Table 1**). Four of these, *Cyp51*, *Lss*, *StarD4*, and *Ctsd*, were represented twice, because of the presence of two independent probes for the same gene on the microarray. Eleven of the 44 genes encode enzymes directly involved in cholesterol synthesis, 3 function as regulators of cholesterol synthesis, 7 are involved in fatty acid synthesis or metabolism, 2 are lipid transporters, 5 represent anonymous cDNAs, and 16 are genes with miscellaneous functions. The fold increase detected by the microarray analysis for most of the genes was generally 1.5–2.5. This relatively modest difference between the *Bpa*$^{1H}$ and *wt* cells was attributable in part to the fact that the *wt* cells

TABLE 1. Genes upregulated in *Bpa*$^{1H}$ cells in LDS

| Gene | GenBank Accession Number | Gene Product | One-Sided *P* | Fold Increase | Function |
|---|---|---|---|---|---|
| *Fdft1*[a] | NM_01019 | Farnesyl diphosphate farnesyl transferase 1 | 9.95E-08 | 2.05 | Cholesterol synthesis |
| *Mvd*[a] | NM_138656 | Mevalonate pyrophosphate decarboxylase | 2.86E-07 | 3.07 | Cholesterol synthesis |
| *Sqle* | NM_009270 | Squalene epoxidase | 3.04E-06 | 1.98 | Cholesterol synthesis |
| *Sc4mol*[a] | NM_025436 | Sterol-C4-methyl oxidase-like | 3.94E-06 | 2.21 | Cholesterol synthesis |
| *Cyp51* | BC031813 | Lanosterol 14α demethylase | 6.16E-06 | 2.08 | Cholesterol synthesis |
| *Acly* | XM_126704 | ATP citrate lyase | 1.01E-05 | 1.88 | Fatty acid synthesis |
| *Sparcl1*[a] | NM_010097 | SPARC-like 1, hevin, SC1 | 2.52E-05 | 1.85 | Matricellular protein |
| *Acat2* | BC012496 | Acyl-CoA:cholesterol acyl transferase 2 | 3.35E-05 | 1.74 | Fatty acid synthesis |
| *Hmgcr*[a] | XM_127496 | 3-Hydroxy-3-methylglutaryl CoA reductase | 3.88E-05 | 1.56 | Cholesterol synthesis |
| *Lce* | NM_130450 | Long-chain fatty acyl elongase | 4.16E-05 | 1.91 | Fatty acid synthesis |
| *Srebp2*[a] | U12330 | Sterol-regulatory element binding protein 2 | 4.33E-05 | 1.53 | Cholesterol regulation |
| *StarD4*[a] | AK014587 | START domain-containing 4 | 4.48E-05 | 1.76 | Cholesterol transport |
| *Cyp51* | NM_020010 | Lanosterol 14a demethylase | 6.39E-05 | 1.68 | Cholesterol synthesis |
| *Hsd17b7* | NM_010476 | Hydroxysteroid 17-β dehydrogenase 7 | 6.52E-05 | 2.07 | Cholesterol synthesis |
| Unknown | NM_026708 | Homology to longevity assurance gene (Lag1) | 6.58E-05 | 1.84 | Ceramide regulation? |
| *Orf11*[a] | NM_021446 | Open reading frame 11 (erg28) | 7.13E-05 | 1.99 | Cholesterol regulation |
| *Fads1* | NM_146094 | Fatty acid desaturase 1 | 7.53E-05 | 1.83 | Fatty acid synthesis |
| *Scd1* | BC007474 | Stearoyl-CoA desaturase 1 | 8.98E-05 | 1.85 | Fatty acid synthesis |
| *Dhcr7*[a] | NM_007856 | 7-Dehydrocholesterol reductase | 9.43E-05 | 2.45 | Cholesterol synthesis |
| *Pcyt2* | NM_024229 | CTP:phosphocholine cytidylyltransferase | 9.43E-05 | 1.71 | Phospholipid synthesis |
| *Epb7.2*[b] | NM_013515 | Erythrocyte protein band 7.2, stomatin | 9.84E-05 | 1.53 | Lipid raft protein |
| *StarD4*[a] | BC005642 | START domain-containing 4 | 1.21E-04 | 1.83 | Cholesterol transport |
| *H2-D1* | BC023409 | MHC class I heavy chain precursor | 1.37E-04 | 1.52 | Histocompatibility antigen |
| Unknown | CA569887 | Unknown | 1.58E-04 | 1.56 | Unknown |
| *Fdps*[a] | NM_134469 | Farnesyl pyrophosphate synthase | 1.80E-04 | 1.74 | Cholesterol synthesis |
| *Cd1d1* | NM_007639 | CD1d1 antigen | 1.82E-04 | 1.53 | Lipid antigen binding |
| *Grina* | NM_023168 | NMDA receptor glutamate binding chain | 1.92E-04 | 1.72 | Receptor |
| Unknown[b] | BG075096 | Unknown | 2.12E-04 | 2.26 | Unknown |
| *Scd2* | NM_009128 | Stearoyl-CoA desaturase 2 | 2.45E-04 | 1.51 | Fatty acid synthesis |
| *Ldlr* | BC019207 | Low density lipoprotein receptor | 2.45E-04 | 1.50 | Cholesterol transport |
| *Lss*[a] | NM_146006 | Lanosterol synthase | 2.67E-04 | 1.92 | Cholesterol synthesis |
| Unknown[b] | XM_131685 | Unknown | 2.72E-04 | 1.54 | Unknown |
| *Mdk* | NM_010984 | Midkine | 3.04E-04 | 1.51 | Growth factor |
| *Atf4* | NM_009716 | Activating transcription factor 4 (CREB2) | 3.06E-04 | 1.66 | Multiple regulatory pathways |
| *Lss*[a] | AK014742 | Lanosterol synthase | 3.09E-04 | 1.78 | Cholesterol synthesis |
| *Fads2* | BC057189 | Fatty acid desaturase 2 | 3.28E-04 | 1.58 | Fatty acid synthesis |
| *Cdkn1c* | NM_009876 | Cyclin-dependent kinase inhibitor 1C | 3.56E-04 | 1.84 | Unknown |
| Unknown | NM_029083 | Unknown | 3.99E-04 | 1.50 | Unknown |
| *Ctsd* | NM_009983 | Cathepsin D | 4.22E-04 | 1.71 | Aspartate protease |
| *Dusp9* | NM_029352 | Dual-specificity phosphatase 9, MPK4 | 4.41E-04 | 1.68 | Mitogen-activated protein kinase phosphatase |
| *Ctsd* | NM_009983 | Cathepsin D | 4.72E-04 | 1.75 | Aspartate protease |
| *Kap* | NM_010594 | Kidney androgen-regulated gene | 5.38E-04 | 1.80 | Unknown |
| *Insig1*[a] | NM_153526 | Insulin-induced gene 1 | 5.81E-04 | 1.66 | Cholesterol regulation |
| *Mef2c* | BC037731 | Myocyte enhancer factor 2C | 6.53E-04 | 1.59 | Muscle development |
| *DMR-N9* | XM_133223 | *Dystrophia myotonica*-linked gene N9 | 7.31E-04 | 1.58 | Unknown |
| *Map17*[a] | NM_026018 | Membrane-associated protein 17 | 7.35E-04 | 2.87 | Cholesterol regulation? |
| *Dgl1, Ypel1* | NM_023249 | Yippee-like 1, cyclophilin-like | 8.86E-04 | 1.81 | Cell morphology? |
| *Ebp* | NM_007898 | Sterol-D8,D7-isomerase | 9.92E-04 | 1.62 | Cholesterol synthesis |

*Bpa*, bare patches; LDS, lipid-depleted serum.
[a] Upregulation confirmed by real-time PCR analysis.
[b] Upregulation not confirmed by real-time PCR analysis.



Downloaded from www.jlr.org by guest, on June 14, 2012

Supplemental Material can be found at:
http://www.jlr.org/content/suppl/2005/12/01/M400462-JLR200.DC2.html
http://www.jlr.org/content/suppl/2005/05/18/M400462-JLR200.DC1.html

also induced cholesterogenic genes when grown in LDS, as demonstrated by real-time PCR results (see below), thus partially masking the total increase in the expression of these genes in the mutant cells.

In contrast to the upregulated genes, those showing significant downregulation in the combined data from the three LDS time points did not show a clear bias toward a specific cellular function or pathway. The top-ranked 49 genes out of 77 that were downregulated with a one-sided *P* value of <0.001 are listed in **Table 2**. Only two of the genes, *Cav1* and *Abca1*, encode proteins with known lipid-related functions. The ABCA1 protein is a membrane-spanning lipid transporter involved in cholesterol efflux from cells (29). As shown by real-time PCR below, significant downregulation of this gene was found exclusively in *Bpa*$^{1H}$ cells, likely reflecting attempts to conserve existing cellular cholesterol. Downregulation of *Cav1*, the main structural protein of caveolae (30), was not confirmed by real-time PCR (see below). Several of the downregulated genes encode cell cycle regulators, including *Pcna*, *Rras*, *Ccnd*, and *Cks2*, probably indicating a secondary response to the increasing stress of cholesterol deficiency on the mutant cells. Interestingly, the oligomer representing the alternative 3′ untranslated region of *Ywhaz* was again the probe with the most significant level of downregulation in the LDS-treated cells, as it was in the samples grown in

TABLE 2. Genes downregulated in *Bpa*$^{1H}$ cells in LDS

| Gene | GenBank Accession Number | Gene Product | One-Sided *P* | Fold Decrease | Function |
|---|---|---|---|---|---|
| *Ywhaz*[a] | XM_147897 | 14-3-3ζ | 6.10E-06 | 4.38 | Phosphoprotein regulation |
| *Epcs3* | NM_025310 | FtsJ homolog 3 | 1.08E-05 | 1.60 | Unknown |
| *Chst1* | NM_023850 | Carbohydrate (keratan sulfate) sulfotransferase 1 | 1.72E-05 | 1.64 | Sulfotransferase |
| Unknown | AL832353 | Unknown | 1.97E-05 | 1.88 | Unknown |
| *Cmkor1*[b] | BC015254 | Chemokine orphan receptor 1 | 2.82E-05 | 1.89 | G-protein-coupled receptor |
| *Usp39* | NM_138592 | Ubiquitin-specific protease 39 | 5.87E-05 | 1.50 | Protein catabolism |
| *Tfdp1* | XM_134001 | Transcription factor Dp-1 | 6.05E-05 | 1.55 | Cell cycle control, E2F binding |
| Unknown [a] | XM_126276 | Unknown | 7.54E-05 | 2.23 | Unknown |
| *Amd1* | NM_009665 | *S*-Adenosylmethionine decarboxylase 1 | 7.97E-05 | 2.16 | Polyamine synthesis |
| *Slbp* | NM_009193 | Stem-loop binding protein | 8.70E-05 | 1.63 | mRNA processing |
| *Cav1*[b] | BC_038280 | Caveolin 1 | 1.06E-04 | 1.70 | Lipid raft structure |
| *Nol5a* | NM_024193 | Nucleolar protein 5a | 1.06E-04 | 1.65 | Ribosome biogenesis |
| *Camk2g* | XM_127599 | Calcium/calmodulin-dependent protein kinase 2γ | 1.27E-04 | 1.56 | Calmodulin binding |
| *AbcA1* [a] | NM_005502 | ATP binding cassette A1 | 1.35E-04 | 2.86 | Cholesterol efflux |
| *Pcna* | NM_011045 | Proliferating cell nuclear antigen | 1.43E-04 | 1.81 | Cell cycle control |
| Unknown [a] | NM_026515 | Unknown | 1.46E-04 | 3.74 | Unknown |
| Unknown | BM220702 | Unknown | 1.51E-04 | 1.66 | Unknown |
| *Prkab2* | BG076307 | Protein kinase, AMP-activated β2 | 1.59E-04 | 1.68 | Metabolic stress response |
| *Cacybp* | XM_129572 | Calcyclin binding protein | 1.65E-04 | 1.76 | Unknown |
| Unknown | NM_152812 | Unknown | 1.73E-04 | 1.61 | Unknown |
| *Cycs* | XM_131904 | Cytochrome C, somatic | 1.74E-04 | 1.69 | Apoptotic signaling cascade |
| *Ranbp1* | NM_011239 | RAN binding protein 1 | 1.75E-04 | 1.50 | Nucleotide hydrolysis of RAN-GTP |
| *Perp* | NM_022032 | p53 apoptosis effector related to Pmp22 | 1.76E-04 | 1.65 | p53-activated apoptosis |
| *Ppfibp1* | BC035209 | PTPRF-interacting protein, binding protein 1 | 1.82E-04 | 1.53 | Unknown |
| *Eif2s1* | NM_026114 | Eukaryotic translation initiation factor 2, subunit 1α | 2.24E-04 | 1.58 | Protein synthesis |
| Unknown | NM_027432 | Unknown | 2.68E-04 | 1.69 | Unknown |
| *Kpnb3* | XM_127872 | Karyopherin (importin) β3 | 2.71E-04 | 1.61 | Protein nuclear import |
| *Rnasep2* | NM_019428 | RNase P2 (Rpp30) | 2.72E-04 | 1.74 | Ribosome component |
| *G3bp* | NM_013716 | Ras-GTPase-activating protein | 2.84E-04 | 1.50 | Ras signaling, stress response |
| *Bmp4* | BC034053 | Bone morphogenetic protein 4 | 3.63E-04 | 1.72 | Cell fate/development |
| *Tardbp* | NM_145556 | TAR DNA binding protein | 3.74E-04 | 1.51 | Transcriptional repression |
| *Ran* | NM_009391 | RAN GTPase | 4.17E-04 | 1.65 | Cell cycle, spindle assembly |
| *Adm* | NM_009627 | Adrenomedullin | 4.27E-04 | 1.63 | Vasodilator |
| Unknown | NM_027093 | Unknown | 4.36E-04 | 1.55 | Unknown |
| *Rrm2* | XM_122396 | Ribonucleotide reductase M2 | 4.45E-04 | 2.35 | Deoxyribonucleotide metabolism |
| *Ppih* | BC016565 | Peptidyl prolyl isomerase (cyclophilin) H | 4.55E-04 | 1.51 | Spliceosome, protein folding |
| Unknown | NM_146169 | Unknown | 4.67E-04 | 1.61 | Unknown |
| *Snrpa1* | NM_021336 | Small nuclear ribonucleoprotein polypeptide A | 4.68E-04 | 1.98 | Ribonucleoprotein complex |
| *Psma2* | NM_008944 | Proteosome subunit, α type 2 | 4.77E-04 | 1.56 | Protein catabolism |
| *Rras2* | NM_025846 | Related RAS viral oncogene homolog | 4.83E-04 | 1.69 | Cell cycle control |
| *Thoc1* | BC027149 | THO complex 1 | 5.04E-04 | 1.54 | mRNA processing/transport? |
| Unknown | BG073324 | Unknown | 5.09E-04 | 1.54 | Unknown |
| *Mcm3* | BC031700 | Minichromosome maintenance-deficient 3 | 5.09E-04 | 1.50 | DNA replication |
| *Hmgb2* | XM_135612 | High-mobility group box 2 | 5.11E-04 | 2.34 | Chromatin structure |
| *Tfpi* | NM_023249 | Tissue factor pathway inhibitor | 5.12E-04 | 1.65 | Protease inhibitor |
| *Ccnd1* | NM_007631 | Cyclin D1 | 5.15E-04 | 1.61 | Cell cycle control |
| *Anxa3* | NM_013470 | Annexin A3 | 5.16E-04 | 1.63 | Phospholipase inhibitor |
| Unknown | XM_134164 | Unknown | 5.31E-04 | 1.60 | Unknown |
| *Cks2* | NM_025415 | CDC28 protein kinase regulatory subunit 2 | 5.53E-04 | 2.22 | Cell cycle regulation |

[a] Downregulation confirmed by real-time PCR analysis.
[b] Downregulation not confirmed by real-time PCR analysis.



Downloaded from www.jlr.org by guest, on June 14, 2012

Supplemental Material can be found at:
http://www.jlr.org/content/suppl/2005/12/01/M400462-JLR200.DC2.html
http://www.jlr.org/content/suppl/2005/05/18/M400462-JLR200.DC1.html

normal medium. No other gene probe showed significant differences in levels between *Bpa*$^{1H}$ and *wt* cells in both normal and LDS media.

### Confirmation of expression differences by real-time PCR

Twenty-four genes from among the upregulated and downregulated genes were assayed by real-time PCR using RNA samples from *wt* and *Bpa*$^{1H}$ MEFs grown in normal or LDS medium for 24 h (Tables 1 and 2). We chose to examine RNA samples from the 24 h LDS time point with the goal of confirming early or primary events resulting from NSDHL deficiency. Of the 24 genes tested, 19 (79%) demonstrated a reproducible change in expression similar to that seen by microarray analysis. The real-time PCR results showed that, as expected, cholesterogenic genes were also induced when the *wt* MEFs were grown in LDS medium, but among the 19 genes confirmed as upregulated by real-time PCR, the *Bpa*$^{1H}$ MEFs always had a greater induction under the same conditions (**Fig. 4A**).

The differential expression pattern exhibited by the anonymous expressed sequence tag NM_026708 was similar to that of multiple lipogenic genes (Fig. 4A). Similarly, the confirmed downregulation of two additional anonymous expressed sequence tags paralleled that of the *Abca1*

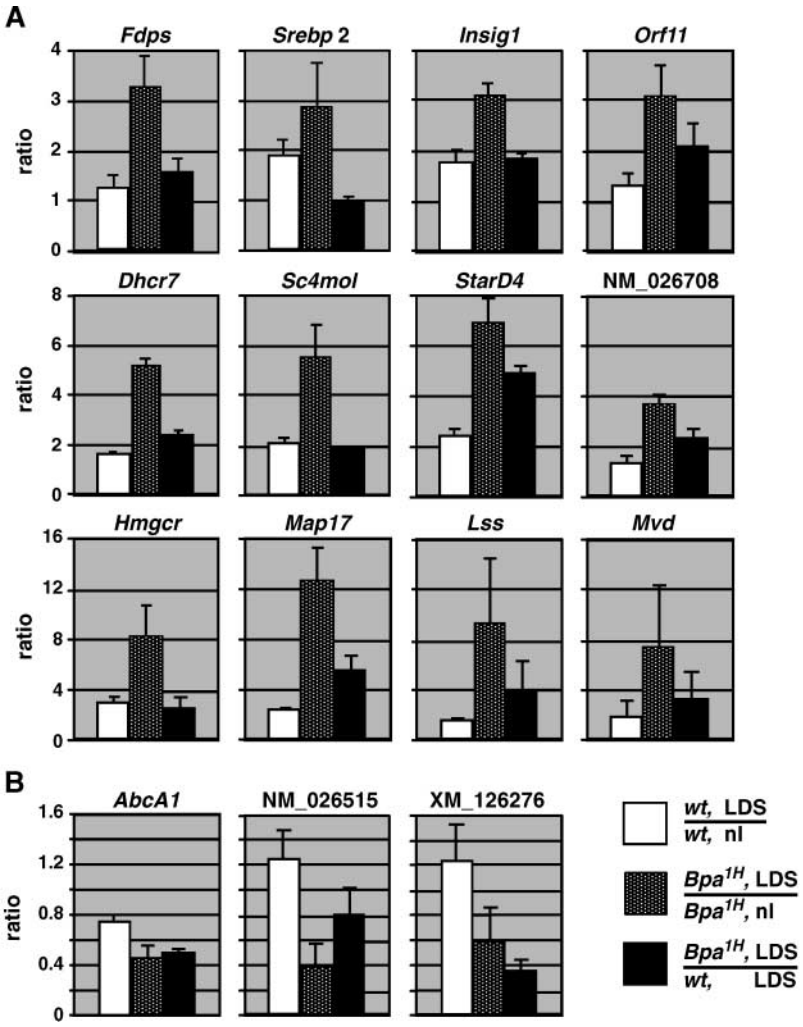


**Fig. 4.** Real-time PCR analysis of gene expression in *Bpa*$^{1H}$ and *wt* MEFs cultured in normal (nl) and LDS media for 24 h. Ratios are shown for RNA samples 2W and 2B that were also used for microarray analysis and represent results from a single experiment performed in triplicate. The ratios shown represent means ± SD and were calculated from values that had been normalized to the signal for *wt* cells in normal medium, which was arbitrarily set to 1. Similar results were obtained for an independent set of RNA samples (1B and 1W) obtained from primary cultures grown in parallel with but not used for microarrays. Although the *Bpa*/*wt* expression ratios were qualitatively similar between the two sets of cDNAs, the magnitude of expression differences varied substantially for some of the genes (not shown) and could reflect normal biologic variability, given the modest expression differences detected by microarrays. A: Graphic representation of the relative mRNA abundance for 12 genes in *wt* cells grown in LDS versus normal media (white bars), *Bpa*$^{1H}$ cells grown in LDS versus normal media (hatched bars), and *Bpa*$^{1H}$ cells in LDS versus *wt* cells in LDS (black bars). These genes had been shown by microarray analysis to be upregulated in *Bpa*$^{1H}$ versus *wt* cells after 24 h in LDS medium. B: Graphic representation, as described for A, of three genes that were identified by microarray analysis as downregulated in *Bpa*$^{1H}$ versus *wt* cells after 24 h in LDS medium.



Downloaded from www.jlr.org by guest, on June 14, 2012

Supplemental Material can be found at:
http://www.jlr.org/content/suppl/2005/12/01/M400462-JLR200.DC2.html
http://www.jlr.org/content/suppl/2005/05/18/M400462-JLR200.DC1.html

transporter gene involved in cellular cholesterol efflux will allow further investigation into whether other cell types, including those affected in heterozygous embryos and adults, demonstrate a selective advantage for cells expressing the *wt Nsdhl* allele.

(Fig. 4B). However, additional experiments will be required to determine whether the functions of these anonymous expressed sequence tags are, indeed, related to lipid metabolism. The unique pattern of downregulation of the alternative 3′ untranslated region transcript from *Ywhaz* that was detected by microarray analysis was confirmed by real-time PCR. The level of the *Ywhaz* transcript was not sensitive to growth in LDS medium in either *wt* or *Bpa*$^{1H}$ MEFs. However, its levels were several orders of magnitude lower in the mutant cells than in *wt* cells, with a threshold cycle of 31 in mutant cells and 19 in *wt* cells. *Hprt* transcript levels, which would not be expected to vary in the four samples, were analyzed as a control for the efficiency of cDNA synthesis among the samples and showed essentially identical amplification curves (data not shown).

## DISCUSSION

Mutations in the murine *Nsdhl* gene are lethal in hemizygous males from early postimplantation to E13.5, depending on the allele. The most consistent defect observed in embryos that progress beyond E9.5 is a poorly developed placenta, specifically in the labyrinth, where embryonic blood vessels fail to invade the trophoblast layer and proliferate to provide an interface for gas and nutrient exchange with maternal blood sinuses (13). Total sterol and cholesterol levels are equivalent between mutant and *wt* embryos, suggesting that the lethality is not caused by simple cholesterol deficiency.

To begin to investigate disease pathogenesis, we screened for changes in gene expression in fibroblasts cultured from *Bpa*$^{1H}$ embryos, taking advantage of an X-linked GFP transgene and random X inactivation to isolate pure populations of *Bpa*$^{1H}$ MEFs. The ratio of GFP+ to GFP− MEFs in the initial unsorted cultures was not significantly different between *wt* and mutant embryos, indicating that the subpopulation expressing the mutant *Bpa*$^{1H}$ null allele proliferated at approximately the same rate as *wt* fibroblasts in the functionally mosaic female embryos, at least until E15.5. When cultured in normal medium, sorted populations of *Bpa*$^{1H}$ MEFs also appeared morphologically normal and grew at a rate comparable to *wt* cells. When cultured in LDS medium, however, the mutant MEFs showed substantial cell death by 48 h, presumably as a result of cholesterol deficiency, whereas *wt* cells continued to grow normally. In contrast, when unsorted populations of GFP+ and *Bpa*$^{1H}$ MEFs were cultured in LDS medium, cell death was not observed, and no change in the ratio of GFP+ to GFP− cells was seen after 72 h (data not shown), suggesting that cells expressing the *Bpa*$^{1H}$ *Nsdhl* allele were rescued by cholesterol synthesized and exported by cells expressing the *wt* allele. The apparent ability of *wt* MEFs to provide sufficient cholesterol for the survival of *Bpa*$^{1H}$ cells would explain the lack of negative selection against *Bpa*$^{1H}$ fibroblasts seen in the E15.5 embryos. The use of the X-linked GFP transgene as an in vivo marker

Finally, the death of *Nsdhl* null fibroblasts after 48 h of culture in LDS medium strongly suggests that the lanosterol derivatives that accumulate in these cells cannot support one or more vital functions of cellular cholesterol and/or that they themselves are toxic. In contrast, fibroblasts from several Smith-Lemli-Opitz patients homozygous for null alleles of *DHCR7* survived for at least 1 week when cultured in LDS medium, suggesting that 7-dehydrocholesterol (7DHC) can substitute for at least some key functions of cholesterol, including maintaining the integrity of cell membranes (31).

Based on homology with yeast, it is predicted that the NSDHL protein would function in a complex with a sterol C-4 methyloxidase, encoded by the *SC4MOL* gene in human (32), and a 3β-ketosterol reductase. During the course of our studies, Marijanovic et al. (33) demonstrated that the protein encoded by the human *HSD17B7* locus functions as a cholesterol biosynthetic 3-ketosterol reductase. In *Saccharomyces cerevisiae*, the *ERG28* gene encodes a regulatory protein for the complex that may act as a scaffold and anchor the C-4 demethylase enzymes to the ER membrane (34, 35). Consistent with this model, our results showed upregulation of *Sc4mol*, *Hsd17b7*, and *Orf11*, the murine ortholog of *ERG28* (34), in *Bpa*$^{1H}$ cells grown in LDS. The increased expression of *Orf11* provides the first functional evidence for a conserved role of the protein in mammalian cholesterol metabolism.

An initial question in understanding the pathogenesis associated with inherited defects in cholesterol biosynthesis is determining how the cell responds to both a deficiency of cholesterol and an abnormal accumulation of specific sterol intermediates at the blocked step in the pathway. Analysis of cultured human fibroblasts isolated from Smith-Lemli-Opitz patients that carry mutations in the *DHCR7* gene showed that when 7DHC levels are significantly increased upon prolonged culture in delipidated medium, the activity of HMGR is suppressed, despite the presence of significantly lower total sterol levels in the mutant cells (31). Indeed, 7DHC was more effective in suppressing HMGR than cholesterol itself. Similarly, mice that are homozygous for a targeted null allele of *Dhcr7*, in which tissue cholesterol is decreased 5- to 6-fold and 7DHC is increased 30- to 40-fold, demonstrate decreased levels of HMGR protein and activity, probably as a result of accelerated proteolysis of the enzyme (36). Levels of mRNA for several cholesterol regulatory proteins and biosynthetic enzymes, including HMGR, remain unchanged between *Dhcr7*$^{-/-}$ and *wt* animals. In contrast, cultured fibroblasts from patients with deficiency of mevalonate kinase, the enzyme subsequent to HMGR in the pathway, accumulate excess mevalonate and demonstrate a 6-fold increase in HMGR activity (20). Thus, mutant cells may show distinct responses to disruption of cholesterol biosynthesis depending on which step in the pathway is affected. Our analysis of *Bpa*$^{1H}$ MEFs showed that, un-



Downloaded from www.jlr.org by guest, on June 14, 2012

Supplemental Material can be found at:
http://www.jlr.org/content/suppl/2005/12/01/M400462-JLR200.DC2.html
http://www.jlr.org/content/suppl/2005/05/18/M400462-JLR200.DC1.html

like *Dhcr7* mutants, loss of NSDHL function caused higher expression of 11 cholesterogenic enzymes, including HMGR, even after 24 h of growth in LDS medium. There was also a concomitant upregulation of genes for seven enzymes involved in fatty acid metabolism. Upregulation of fatty acid biosynthetic enzymes was reported in transgenic mice overexpressing sterol-regulatory element binding protein 2 (SREBP2) (37, 38), consistent with the lack of absolute specificity of SREBP1 and SREBP2 for fatty acid and cholesterol biosynthetic genes, respectively (38, 39).

In addition to the lipogenic enzymes, we detected modestly increased expression of the two regulatory genes, *Srebp2* and *Insig1*. *Srebp1* was not represented in the array, whereas expression of *Insig2* was unchanged (data not shown). The upregulation of *Srebp2* may account for the increased expression of the cholesterol biosynthetic enzymes, as well as the LDL receptor, because most of these genes have been shown to be direct targets of transcriptional activation by SREBP2 (37–41). Although our study did not measure levels of nuclear SREBP2 in the MEFs, it has been demonstrated that SREBP2 activation and nuclear import is stimulated by cholesterol depletion (reviewed in 1, 2). Thus, we hypothesize that the higher level of *Srebp2* mRNA in $Bpa^{1H}$ versus *wt* MEFs in LDS is responsible for or at least contributes to the increased expression of cholesterogenic enzymes observed in these cells. The observed increased expression of *Insig1* was somewhat surprising given that the sterol-mediated binding of INSIGs to SREBP cleavage-activating protein (SCAP) results in the retention of inactive SREBPs in the ER (42). However, the expression of *Insig1* itself is directly upregulated by SREBPs, whereas *Insig2* is insensitive to regulation by SREBPs, except in the liver. Thus, the increased expression of *Srebp2* observed in $Bpa^{1H}$ MEFs may account for the modest upregulation of *Insig1* without concomitant increased expression of *Insig2*.

Among the genes showing upregulation in $Bpa^{1H}$ MEFs were two, *Map17* and *StarD4*, that encode proteins whose precise function is unclear but have previously been implicated in cholesterol metabolism. MAP17 (for membrane-associated protein 17) plays a regulatory role in the uptake of HDL cholesterol through its interaction with PDZK1 in the liver (43). Among several proteins known to associate with PDZK1 at the plasma membrane is scavenger receptor class B type I, the receptor that mediates both the uptake of HDL cholesterol in the liver and cholesterol efflux from a variety of peripheral cell types (reviewed in 44). Overexpression of MAP17 in the livers of transgenic mice results in 2-fold increased plasma cholesterol levels and dramatic reductions in the scavenger receptor class B type I and PDZK1 proteins (43). MAP17 transcript levels are increased in livers of transgenic mice that overexpress either SREBP-1a or SREBP-2, but not in *Scap* knockout mice, suggesting that the MAP17 gene is either a direct or indirect target of SREBPs (38).

STARD4 is a member of the START domain family of proteins based on its homology to STAR (for steroidogenic acute regulatory protein), a protein that binds cholesterol and participates in its translocation from the outer to the inner mitochondrial membrane in steroidogenic cells (reviewed in 45). The gene was initially identified by microarray analysis as downregulated in livers of mice fed a high-cholesterol diet (41, 46). Although the exact function of the protein remains unknown, *Stard4* expression in mouse 3T3-L1 cells decreases in the presence of increased levels of exogenous cholesterol and increases in the presence of lovastatin, suggesting a role in cholesterol homeostasis (46). Furthermore, the gene appears to be a direct target of SREBP regulation based on its increased expression in the livers of transgenic mice that overexpress SREBP and in *Scap* knockout mice (38).

Finally, one can envision how several of the other upregulated genes might be perturbed by a complete block in cholesterol biosynthesis. Cathepsin D is an endosomal aspartate protease that is activated by the sphingolipid ceramide and plays a role in ceramide-induced apoptosis as well as in epidermal differentiation (47, 48). Ceramide is generated in response to a variety of stress conditions and signaling molecules and influences cellular proliferation, differentiation, and apoptosis (reviewed in 49). Ceramide may also affect cell function through its role in membrane structure and microdomains at the Golgi, endosomes, and plasma membrane (reviewed in 50). The predicted amino acid sequence of one of the anonymous cDNAs identified as upregulated in our microarray analysis (NM_026708) showed 42% sequence similarity (E-value of 1E-18) to a domain in the yeast *Lag1* gene that functions in ceramide synthesis (51–53).

In light of the fully penetrant early lethality of the $Bpa^{1H}$ mutation in hemizygous males, our microarray analysis showed surprisingly few differences in gene expression between mutant and *wt* cells when the MEFs were cultured in normal serum. This result suggests that the abnormalities seen in vivo arise from cellular defects that are not associated with dramatic changes in mRNA level, that localized cholesterol deficiency may in fact occur in a subset of tissues of the mutant embryo but is not detectable by sterol analysis of the whole embryo, or that embryonic fibroblasts derived from midgestation embryos are less sensitive to the loss of NSDHL function than other cell types of the earlier, gastrulating embryo. Finally, the sorted $Bpa^{1H}$ MEFs used in this study will provide a unique and valuable tool for the in vitro analysis of possible perturbation of lipid raft structure, intracellular sterol trafficking, or signaling pathways.

The authors thank Dr. Hugo Caldas and Cindy McAllister for help with the FACS analyses, Dr. David Armbruster and the Columbus Children's Research Institute Microarray Core for performing the microarray analyses, and Dr. David Burke (University of Michigan) for providing GFP transgenic mice. This work was supported by National Institutes of Health Grant R01 HD-38572 to G.E.H.

## REFERENCES

1. Horton, J. D., J. L. Goldstein, and M. S. Brown. 2002. SREBPs: activators of the complete program of cholesterol and fatty acid synthesis in the liver. *J. Clin. Invest.* **109:** 1125–1131.



Downloaded from www.jlr.org by guest, on June 14, 2012

Supplemental Material can be found at:
http://www.jlr.org/content/suppl/2005/12/01/M400462-JLR200.DC2.html
http://www.jlr.org/content/suppl/2005/05/18/M400462-JLR200.DC1.html

2. Hampton, R. Y. 2002. Proteolysis and sterol regulation. *Annu. Rev. Cell Dev. Biol.* **18:** 345–378.
3. Maxfield, F. R., and D. Wustner. 2002. Intracellular cholesterol transport. *J. Clin. Invest.* **110:** 891–898.
4. Simons, K., and R. Ehehalt. 2002. Cholesterol, lipid rafts, and disease. *J. Clin. Invest.* **110:** 597–603.
5. Mann, R. K., and P. A. Beachy. 2004. Novel lipid modifications of secreted protein signals. *Annu. Rev. Biochem.* **73:** 891–923.
6. Porter, F. D. 2003. Human malformation syndromes due to inborn errors of cholesterol synthesis. *Curr. Opin. Pediatr.* **15:** 607–613.
7. Herman, G. E. 2003. Disorders of cholesterol biosynthesis: prototypic metabolic malformation syndromes. *Hum. Mol. Genet.* **12:** R75–R88.
8. Wechsler, A., A. Brafman, M. Shafir, M. Heverin, H. Gottlieb, G. Damari, S. Gozlan-Kelner, I. Spivak, O. Moshkin, E. Fridman, et al. 2003. Generation of viable cholesterol-free mice. *Science.* **302:** 2087.
9. Liu, X. Y., A. W. Dangel, R. I. Kelley, W. Zhao, P. Denny, M. Botcherby, B. Cattanach, J. Peters, P. R. Hunsicker, A. M. Mallon, et al. 1999. The gene mutated in bare patches and striated mice encodes a novel 3beta-hydroxysteroid dehydrogenase. *Nat. Genet.* **22:** 182–187.
10. Herman, G. E. 2000. X-linked dominant disorders of cholesterol biosynthesis in man and mouse. *Biochim. Biophys. Acta.* **1529:** 357–373.
11. Konig, A., R. Happle, D. Bornholdt, H. Engel, and K. H. Grzeschik. 2000. Mutations in the NSDHL gene, encoding a 3β-hydroxysteroid dehydrogenase, cause CHILD syndrome. *Am. J. Med. Genet.* **90:** 339–346.
12. Lucas, M. E., Q. Ma, D. Cunningham, J. Peters, B. Cattanach, M. Bard, B. K. Elmore, and G. E. Herman. 2003. Identification of two novel mutations in the murine Nsdhl sterol dehydrogenase gene and development of a functional complementation assay in yeast. *Mol. Genet. Metab.* **80:** 227–233.
13. Caldas, H., D. Cunningham, X. Wang, F. Jiang, L. Humphries, R. I. Kelley, and G. E. Herman. 2005. Placental defects are associated with male lethality in bare patches and striated embryos deficient in the NAD(P)H steroid dehydrogenase-like (NSDHL) enzyme. *Mol. Genet. Metab.* **84:** 48–60.
14. Hadjantonakis, A. K., M. Gertsenstein, M. Ikawa, M. Okabe, and A. Nagy. 1998. Non-invasive sexing of preimplantation stage mammalian embryos. *Nat. Genet.* **19:** 220–222.
15. Hadjantonakis, A. K., L. L. Cox, P. P. Tam, and A. Nagy. 2001. An X-linked GFP transgene reveals unexpected paternal X-chromosome activity in trophoblastic giant cells of the mouse placenta. *Genesis.* **29:** 133–140.
16. Simmler, M. C., B. M. Cattanach, C. Rasberry, C. Rougeulle, and P. Avner. 1993. Mapping the murine Xce locus with (CA)n repeats. *Mamm. Genome.* **4:** 523–530.
17. Avner, P., M. Prissette, D. Arnaud, B. Courtier, C. Cecchi, and E. Heard. 1998. Molecular correlates of the murine Xce locus. *Genet. Res.* **72:** 217–224.
18. Mroz, K., T. J. Hassold, and P. A. Hunt. 1999. Meiotic aneuploidy in the XXY mouse: evidence that a compromised testicular environment increases the incidence of meiotic errors. *Hum. Reprod.* **14:** 1151–1156.
19. Angel, T. A., C. J. Faust, J. C. Gonzales, S. Kenwrick, R. A. Lewis, and G. E. Herman. 1993. Genetic mapping of the X-linked dominant mutations striated (Str) and bare patches (Bpa) to a 600-kb region of the mouse X chromosome: implications for mapping human disorders in Xq28. *Mamm. Genome.* **4:** 171–176.
20. Gibson, K. M., G. Hoffmann, A. Schwall, R. L. Broock, S. Aramaki, L. Sweetman, W. L. Nyhan, I. K. Brandt, R. S. Wappner, and W. Lehnert. 1990. 3-Hydroxy-3-methylglutaryl coenzyme A reductase activity in cultured fibroblasts from patients with mevalonate kinase deficiency: differential response to lipid supplied by fetal bovine serum in tissue culture medium. *J. Lipid Res.* **31:** 515–521.
21. Levin, M. L., A. Chatterjee, A. Pragliola, K. C. Worley, M. Wehnert, O. Zhuchenko, R. F. Smith, C. C. Lee, and G. E. Herman. 1996. A comparative transcription map of the murine bare patches (Bpa) and striated (Str) critical regions and human Xq28. *Genome Res.* **6:** 465–477.
22. Brown, P. O. Lab Homepage, Stanford University, Department of Biochemistry. Amino-allyl labeling protocol. (Updated February 3, 2001, at http://cmgm.stanford.edu/pbrown/protocol/aminoallyl.htm.)
23. Yang, Y. H., S. Dudoit, P. Luu, and T. P. Speed. 2001. Normalization for cDNA Microarray Data. SPIE BIOS, San Jose, California.
24. Eisen, M. B., P. T. Spellman, P. O. Brown, and D. Botstein. 1998. Cluster analysis and display of genome-wide expression patterns. *Proc. Natl. Acad. Sci. USA.* **95:** 14863–14868.
25. Carter, M. G., T. Hamatani, A. A. Sharov, C. E. Carmack, Y. Qian, K. Aiba, N. T. Ko, D. B. Dudekula, P. M. Brzoska, S. S. Hwang, et al. 2003. In situ-synthesized novel microarray optimized for mouse stem cell and early developmental expression profiling. *Genome Res.* **13:** 1011–1021.
26. Takahashi, Y. 2003. The 14-3-3 proteins: gene, gene expression, and function. *Neurochem. Res.* **28:** 1265–1273.
27. Wilker, E., and M. B. Yaffe. 2004. 14-3-3 proteins—a focus on cancer and human disease. *J. Mol. Cell. Cardiol.* **37:** 633–642.
28. Maquat, L. E. 2004. Nonsense-mediated mRNA decay: splicing, translation and mRNP dynamics. *Nat. Rev. Mol. Cell Biol.* **5:** 89–99.
29. Knight, B. L. 2004. ATP-binding cassette transporter A1: regulation of cholesterol efflux. *Biochem. Soc. Trans.* **32:** 124–127.
30. Cohen, A. W., R. Hnasko, W. Schubert, and M. P. Lisanti. 2004. Role of caveolae and caveolins in health and disease. *Physiol. Rev.* **84:** 1341–1379.
31. Honda, M., G. S. Tint, A. Honda, L. B. Nguyen, T. S. Chen, and S. Shefer. 1998. 7-Dehydro-cholesterol down-regulates cholesterol biosynthesis in cultured Smith-Lemli-Opitz syndrome skin fibroblasts. *J. Lipid Res.* **39:** 647–657.
32. Li, L., and J. Kaplan. 1996. Characterization of yeast methyl sterol oxidase (ERG25) and identification of a human homologue. *J. Biol. Chem.* **271:** 16927–16933.
33. Marijanovic, Z., D. Laubner, G. Moller, C. Gege, B. Husen, J. Adamski, and R. Breitling. 2003. Closing the gap: identification of human 3-ketosteroid reductase, the last unknown enzyme of mammalian cholesterol biosynthesis. *Mol. Endocrinol.* **17:** 1715–1725.
34. Gachotte, D., J. Eckstein, R. Barbuch, T. Hughes, C. Roberts, and M. Bard. 2001. A novel gene conserved from yeast to humans is involved in sterol biosynthesis. *J. Lipid Res.* **42:** 150–154.
35. Mo, C., M. Valachovic, S. K. Randall, J. T. Nickels, and M. Bard. 2002. Protein-protein interactions among C-4 demethylation enzymes involved in yeast sterol biosynthesis. *Proc. Natl. Acad. Sci. USA.* **99:** 9739–9744.
36. Fitzky, B. U., F. F. Moebious, H. Asaoka, H. Waage-Baudet, L. Xu, G. Xu, N. Maeda, K. Kluckman, S. Hiller, H. Yu, et al. 2001. 7-Dehydrocholesterol-dependent proteolysis of HMG-CoA reductase suppresses sterol biosynthesis in a mouse model of Smith-Lemli-Opitz/RSH syndrome. *J. Clin. Invest.* **108:** 905–915.
37. Horton, J. D., I. Shimomura, M. S. Brown, R. E. Hammer, J. L. Goldstein, and H. Shimano. 1998. Activation of cholesterol synthesis in preference to fatty acid synthesis in liver and adipose tissue of transgenic mice overproducing sterol regulatory element-binding protein-2. *J. Clin. Invest.* **101:** 2331–2339.
38. Horton, J. D., N. A. Shah, J. A. Warrington, N. N. Anderson, S. W. Park, M. S. Brown, and J. L. Goldstein. 2003. Combined analysis of oligonucleotide microarray data from transgenic and knockout mice identifies direct SREBP target genes. *Proc. Natl. Acad. Sci. USA.* **100:** 12027–12032.
39. Edwards, P. A., D. Tabor, H. R. Kast, and A. Venkateswaran. 2000. Regulation of gene expression by SREBP and SCAP. *Biochim. Biophys. Acta.* **1529:** 103–113.
40. Sakakura, Y., H. Shimano, H. Sone, A. Takahashi, K. Inoue, H. Toyoshima, S. Suzuki, and N. Yamada. 2001. Sterol regulatory element-binding proteins induce an entire pathway of cholesterol synthesis. *Biochem. Biophys. Res. Commun.* **286:** 176–183.
41. Maxwell, K. N., R. E. Soccio, E. M. Duncan, E. Sehayek, and J. L. Breslow. 2003. Novel putative SREBP and LXR target genes identified by microarray analysis in liver of cholesterol-fed mice. *J. Lipid Res.* **44:** 2109–2119.
42. Engelking, L. J., H. Kuriyama, R. E. Hammer, J. D. Horton, M. S. Brown, J. L. Goldstein, and G. Liang. 2004. Overexpression of Insig-1 in livers of transgenic mice inhibits SREBP processing and reduces insulin-stimulated lipogenesis. *J. Clin. Invest.* **113:** 1168–1175.
43. Silver, D. L., N. Wang, and S. Vogel. 2003. Identification of small PDZK1-associated protein, DD96/MAP17, as a regulator of PDZK1 and plasma high density lipoprotein levels. *J. Biol. Chem.* **278:** 28528–28532.
44. Connelly, M. A., and D. L. Williams. 2004. Scavenger receptor BI: a scavenger receptor with a mission to transport high density lipoprotein lipids. *Curr. Opin. Lipidol.* **15:** 287–295.

Downloaded from www.jlr.org by guest, on June 14, 2012

Supplemental Material can be found at:
http://www.jlr.org/content/suppl/2005/12/01/M400462-JLR200.DC2.html
http://www.jlr.org/content/suppl/2005/05/18/M400462-JLR200.DC1.html

45. Strauss, J. F., 3rd, T. Kishida, L. K. Christenson, T. Fujimoto, and H. Hiroi. 2003. START domain proteins and the intracellular trafficking of cholesterol in steroidogenic cells. *Mol. Cell. Endocrinol.* **202:** 59–65.
46. Soccio, R. E., and J. L. Breslow. 2004. Intracellular cholesterol transport. *Arterioscler. Thromb. Vasc. Biol.* **24:** 1–12.
47. Egberts, F., M. Heinrich, J-M. Jensen, S. Winoto-Morbach, S. Pfeiffer, M. Wickel, M. Schunck, J. Steude, P. Saftig, E. Proksch, et al. 2004. Cathepsin D is involved in the regulation of transglutaminase 1 and epidermal differentiation. *J. Cell Sci.* **117:** 2295–2307.
48. Heinrich, M., J. Neumeyer, M. Jakob, C. Hallas, V. Tchikov, S. Winoto-Morbach, M. Wickel, W. Schneider-Brachert, A. Trauzold, A. Hethke, et al. 2004. Cathepsin D links TNF-induced acid sphingomyelinase to Bid-mediated cspase-9 and -3 activation. *Cell Death Differ.* **11:** 550–563.
49. Yang, J., Y. Yu, S. Sun, and P. J. Duerksen-Hughes. 2004. Ceramide and other sphingolipids in cellular responses. *Cell Biochem. Biophys.* **40:** 323–350.
50. van Blitterwijk, W. J., A. H. van der Luit, R. J. Veldman, M. Verheij, and J. Borst. 2003. Ceramide: second messenger or modulator of membrane structure and dynamics. *Biochem. J.* **369:** 199–211.
51. Winter, E., and C. P. Ponting. 2002. TRAM, LAG1 and CLN8: members of a novel family of lipid-sensing domains? *Trends Biochem. Sci.* **27:** 381–383.
52. Venkataraman, K., C. Riebeling, J. Bodennec, H. Riezman, J. C. Allegood, M. C. Sullards, A. H. Merrill, Jr., and A. H. Futerman. 2002. Upstream of growth and differentiation factor 1 (*uog1*), a mammalian homolog of the yeast longevity assurance gene 1 (*LAG1*), regulates *N*-stearoyl-sphinganine (C18-(dihydro)ceramide) synthesis in a fumonisin $B_1$-independent manner in mammalian cells. *J. Biol. Chem.* **277:** 35642–35649.
53. Riebeling, C., J. C. Allegood, E. Wang, A. H. Merrill, Jr., and A. H. Futerman. 2003. Two mammalian longevity assurance gene (LAG1) family members, *trh1* and *trh4*, regulate dihydroceramide synthesis using different fatty acyl-CoA donors. *J. Biol. Chem.* **278:** 43452–43459.



Downloaded from www.jlr.org by guest, on June 14, 2012